[3]Chaderjian, N. M., "Transonic Navier-Stokes Wing Solutions Using a Zonal Approach," NASA TM-88248, April 1986.
[4]Buning, P. G., Chiu, I. T., Obayashi, S., Rizk, Y. M., and Steger, J. L., "Numerical Simulation of the Integrated Space Shuttle Vehicle in Ascent," AIAA Paper 88-4359, Aug. 1988.
[5]Srinivasan, G. R., Baeder, J. D., Obayashi, S., and McCroskey, W. J., "Flowfield of a Lifting Hovering Rotor—A Navier-Stokes Simulation," 16th European Rotorcraft Forum, Paper I.3.5, Glasgow, Scotland, UK, Sept. 1990; also NASA TM-102862, Aug. 1990.
[6]Chen, C. L., and McCroskey, W. J., "Numerical Simulation of Helicopter Multi-Bladed Rotor Flow," AIAA Paper 88-0046, Jan. 1988.
[7]Obayashi, S., "Free-Stream Capturing in Fluid Conservation Law for Moving Coordinates in Three Dimensions," NASA CR-177572, Jan. 1991
[8]Thomas, P. D., and Lombard, C. K., "Geometric Conservation Law and Its Application to Flow Computations on Moving Grids," *AIAA Journal*, Vol. 17, No. 10, 1979, pp. 1030–1037.

Semi-Inverse Marching Characteristics Scheme for Supersonic Flows

Joseph Falcovitz* and Allen E. Fuhs†
Naval Postgraduate School, Monterey, California 93941

Nomenclature

$C^{\pm}$ = characteristic lines corresponding to $\theta \pm \mu$
$R^{\pm}$ = Riemann invariants along $C^{\pm}$, $(\nu \mp \theta)$
M = Mach number
x,y = Cartesian coordinates
Γ = $[(\gamma + 1)/(\gamma - 1)]^{1/2}$
γ = specific heats ratio
δ = symmetry index (zero planar flow, one axisymmetric flow)
θ = inclination of flow velocity vector relative to x axis
μ = Mach angle, $\sin \mu = M^{-1}$
ν = Prandtl-Meyer function $\nu(M) = \Gamma \arctan(\Gamma^{-1}\sqrt{M^2 - 1}) - \arctan(\sqrt{M^2 - 1})$

Introduction

THE purpose of this Note is to present a modification of the inverse marching characteristics scheme for compressible flows that is designed to yield an exact computation of centered rarefaction waves, such as the Prandtl-Meyer corner expansion flow (PMF). The key idea is to combine a semi-inverse marching scheme (grid points near corner are located on continuous characteristics emanating from the corner) with the designation of Riemann invariants as flow variables. The resulting semi-inverse marching algorithm (SIMA) scheme replicates a Prandtl-Meyer flow accurately, while yielding the solution on a relatively regular grid. In this Note, the SIMA scheme is presented following a brief discussion of the background and then its accuracy is demonstrated by considering a planar plume flow.

The inverse marching method of characteristics[1] is a standard scheme for the computation of compressible isentropic flow in two dimensions. Two instances of flow are possible: either the time-dependent compressible flow in x,t or the steady supersonic flow in x,y. We shall restrict our discussion to the latter. (The time-dependent case can be treated in a very similar fashion.) To fix ideas, we assume a supersonic exit flow, where the characteristic lines $C^{\pm}$ (corresponding to $\theta \pm \mu$) propagate in the positive y direction as depicted in Fig. 1. (However, if this condition does not hold, lines of y = const may be replaced by a set of curves such that $C^{\pm}$ characteristics propagate forward from every point on each curve.) The advantage of the inverse marching algorithm (IMA) scheme is that it yields a solution on a relatively regular grid of points, whereas the direct method of characteristics[1] renders the flowfield at an irregular grid formed by the intersection of C^- and C^+ characteristic lines and their reflections from boundaries.

The IMA scheme consists in seeking the flow at new grid points (x_{ij},y_j) located on a new row $y = y_j$, where the new row is obtained from an old row by a forward marching step: $y_j = y_{j-1} + \Delta y_{j-1}$. The number and distribution of grid points on each new row is independent of their distribution on the old row. The recommended flow variables are velocity components [Ref. 1, Secs. 12-5(b) and 13-5(a)].

To determine the flow at grid points of a new row, C^- and C^+ characteristics are inversely extended from each new point until they intersect the old row $y = y_{j-1}$ at corresponding C^- or C^+ trace points (Fig. 2). The flow at each new grid point is then obtained from the C^- and C^+ compatibility relations that are approximated by a pair of centered implicit finite difference equations.[1] It has been found that by applying the IMA scheme to a PMF having a uniform supersonic flow on its upstream side, the computed results deviated appreciably from the known analytic (self-similar) solution. The reasons for errors in computing a corner flow by the IMA scheme are well understood. Two factors contribute to these errors:

1) There is an error in locating old trace points by inversely extending $C^{\pm}$ characteristic lines from new grid points.

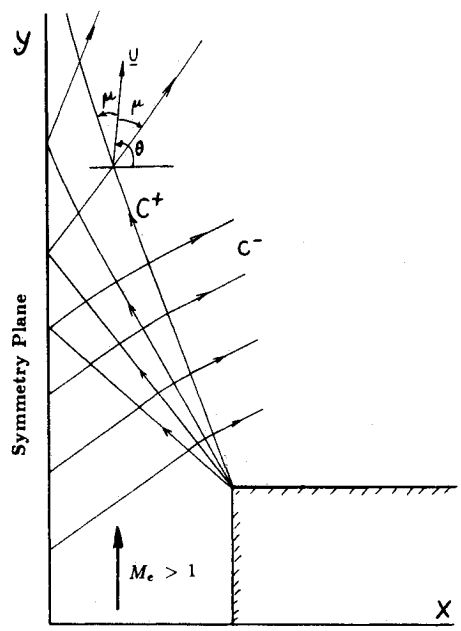

Fig. 1 Reflection of Prandtl-Meyer fan from symmetry plane (schematic).

Received Jan. 8, 1991; revision received June 30, 1991; accepted for publication July 19, 1991. This paper is declared a work of the U.S. Government and is not subject to copyright protection in the United States.

*Senior Research Professor, Space Systems Academic Group; currently, Faculty of Aerospace Engineering, Technion, Haifa, Israel.
†Chairman, Space Systems Academic Group; currently, Distinguished Professor (Emeritus). Fellow AIAA.

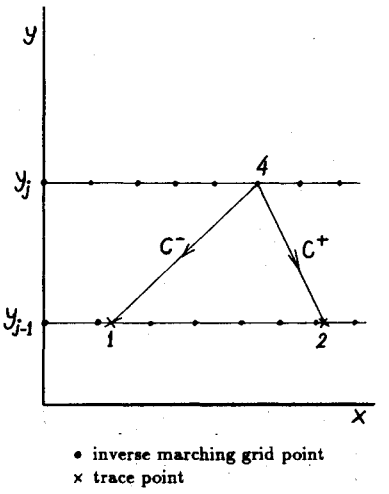

Fig. 2 Inverse marching scheme.

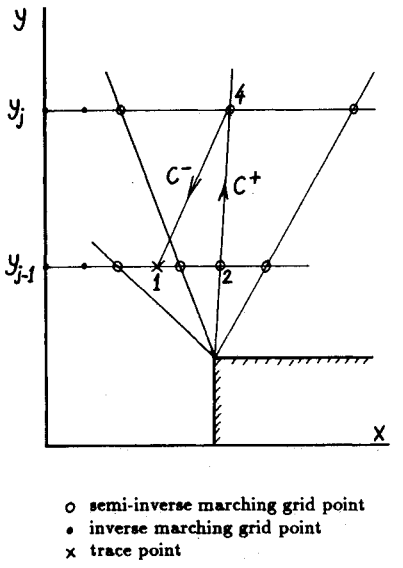

Fig. 3 Semi-inverse marching scheme.

2) There is an additional error in computing the flow variables at each trace point since they are determined by interpolation using values at adjacent old grid points. Both errors are large when the inverse marching starts out from the corner by virtue of the singularity of the inviscid flow solution there. Rather than analyze these errors, we suggest a modified scheme eliminating all errors related to the flow singularity at a sharp expansive corner.

A partial elimination of errors at a corner is obtained by adopting a grid modification that consists in maintaining continuous characteristic lines of a particular family nicknamed the primary family [Ref. 1, Secs. 19-6(a) and 19-6(j)]. Some or all grid points at a new row are obtained as the intersection of primary characteristic lanes extended in a forward direction from old row grid points (Fig. 3). In our sample case, the primary family is C^+ and interpolation at C^+ trace points is thereby eliminated. However, the treatment of C^- lines is identical to that of the IMA scheme, and interpolation errors at C^- trace points remain.

The additional modification needed to eliminate all corner-related interpolation errors is simply the designation of Riemann invariants $(\nu \mp \theta)$ as the flow variables. Interpolation errors are thus completely eliminated in the case of a self-similar corner flow, since in this case the Riemann invariant that requires interpolation is uniform throughout the centered wave region. The resulting SIMA scheme replicates a PMF accurately; it is also expected to yield good numerical solutions to a centered rarefaction wave (CRW) flow that unlike PMF is not self-similar (e.g., axisymmetric flow), since additional terms in the governing equations are smooth at the corner.

Semi-Inverse Marching Algorithm Scheme

The compatibility relations that hold along the characteristic lines $C^{\pm}$ in an axisymmetric (x is the radial coordinate) supersonic isentropic flow[2] are as follows (see also Fig. 2):

Along C^+

$$(\nu - \theta)_4 = (\nu - \theta)_2 + \delta \frac{\sin \mu_{24} \cos \theta_{24}}{x_{24}} \Delta\mu_{24} \tag{1a}$$

Along C^-

$$(\nu + \theta)_4 = (\nu + \theta)_1 + \delta \frac{\sin \mu_{14} \cos \theta_{14}}{x_{14}} \Delta\xi_{14} \tag{1b}$$

where the Riemann invariants are $R^+ = (\nu - \theta)$ and $R^- = (\nu + \theta)$. The Prandtl-Meyer function $\nu(M)$ is related to Mach number as given in the Nomenclature.[2] The centered values $(\cdot)_{24}$ or $(\cdot)_{14}$ are defined in the following manner. All flow variables are functions of $R^{\pm}$ since $\nu = \frac{1}{2}(R^- + R^+)$ and $\theta = \frac{1}{2}(R^- - R^+)$ and since M can be obtained from ν by inverting the Prandtl-Meyer function $\nu(M)$. Therefore, by defining $R_{14}^{\pm}$, $R_{24}^{\pm}$ as the arithmetic mean of $R_1^{\pm}$, $R_2^{\pm}$, and $R_4^{\pm}$, the centered values of M, sin μ, cos θ follow. The increments $\Delta\eta_{24}$, $\Delta\xi_{14}$ denote the length of segments 2,4 and 1,4 respectively (Fig. 2 or Fig. 3), which are computed from the corresponding coordinates; x_{14}, x_{24} are the arithmetic means of the corresponding values of x_1, x_2, and x_4. The only accessory relations needed are the geometrical expressions:

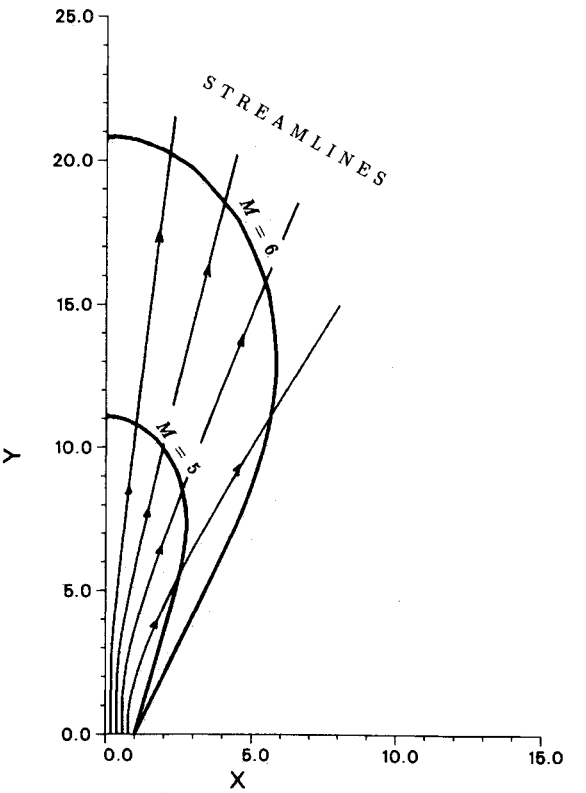

Fig. 4 Prandtl-Meyer flow at $M_e = 3$ and $\gamma = 1.4$.

Along C^-

$$y_j - y_{j-1} = (x_4 - x_1) \tan (\theta_{14} - \mu_{14}) \quad (2a)$$

Along C^+

$$y_j - y_{j-1} = (x_4 - x_2) \tan (\theta_{24} + \mu_{24}) \quad (2b)$$

The computation of flow at a new grid point calls for either the semi-inverse marching algorithm (Fig. 3) or the inverse marching algorithm (Fig. 2), according to whether the particular grid point is located on an extension of a C^+ characteristic. In the code written to implement the SIMA scheme, C^+ characteristics were bypassed automatically when they approached the symmetry line ($x = 0$), and some inverse marching grid points were added between the symmetry line ($x = 0$) and the first C^+ characteristic.[3]

Thus, there are two types of new grid points in the SIMA scheme: the inverse marching type (Fig. 2) and the semi-inverse marching type (Fig. 3). In the inverse marching case, the location x_4 of a new point is determined in advance, and the trace points x_1, x_2 (Fig. 2) are obtained by inversely extending C^- and C^+ characteristics from new point (x_4,y_4); Eqs. (2) are used to get x_1 and x_2. In the semi-inverse marching case (Fig. 3), the location of x_4 is obtained by a forward extension of C^+ from old point (x_2,y_2), and trace point x_1 is obtained by an inverse extension of C^- from new point (x_4,y_4); again, Eqs. (2) are used for computing x_4 and x_1.

The flow at each new grid point of either the inverse or the semi-inverse type is determined by solving the pair of implicit compatibility equations (1). The solution is obtained by iterations that are repeated at each point until convergence is established, the initial guess being given by the interpolated old grid flow variables. For more detailed information, the reader is referred to a report that also contains a plume code listing.[3]

Flow Test Case

As a test of the accuracy of the SIMA scheme, we chose the reflection of a PMF ($\delta = 0$) from a symmetry plane ($x = 0$), which represents a planar plume flow. The flow at $x = 0$ was independently computed by integrating the compatibility equations along characteristic lines fanning out from the corner and their reflections from the symmetry plane, using the direct method of characteristics.[2]

We have done so for the test case of $M_e = 3$, $\gamma = 1.4$, and a fan of C^+ lines chosen with $\Delta M = 0.05$ at the corner; it was verified by numerical convergence that $M(o,y)$ so obtained was practically an exact solution (relative error in Mach number of 10^{-5} or less). A SIMA computation was also performed for the same exit flow, and it is depicted in Fig. 4 (streamlines and lines of const M). The initial grid was comprised of 30 points across the exit plane (inverse points), followed by 30 semi-inverse points corresponding to C^+ lines with $\Delta M = 0.05$ at the corner. The downstream range of $y/x_c = 30$ was reached by about 600 (unequal) steps. The marching steps were limited in such a way that $C^\pm$ trace points would not be more than one old grid interval apart. The SIMA and the exact results were compared by evaluating the relative difference in $M(o,y)$. We found that the relative error in Mach number increased from 0.1% at $y/x_c = 5$ [$M(o,y) = 3.8$] to 0.3% at $y/z_c = 30$ [$M(o,y) = 6.5$], which seems adequate for plume flow computations.

References

[1]Zucrow, M. J., and Hoffman, J. D., *Gas Dynamics*, Wiley, New York, 1976.

[2]Liepmann, H. W., and Roshko, A., *Elements of Gasdynamics*, Wiley, New York, 1957.

[3]Falcovitz, J., "Numerical Computation of Ring-Symmetric Spacecraft Exhaust Plumes," Naval Postgraduate School, Monterey, CA, Rept. NPS 72-87-001CR, Jan. 1987.

Cylinder-Induced Shock-Wave Boundary-Layer Interaction

Oktay Özcan* and Bülent K. Yüceil†
Istanbul Technical University, Istanbul 80626, Turkey

Introduction

THE shock-wave boundary-layer interaction generated by a circular cylinder mounted on a flat plate is a problem of significant academic and practical importance. Korkegi[1] reports that such an interaction can cause structural damage on hypersonic aircraft. A detached bow shock wave is formed ahead of the cylinder. The boundary-layer developing on the flat plate interacts with the bow shock and separates. Sedney and Kitchens[2] and Özcan[3] report that the number of separation lines ahead of the cylinder varies between one and three and is a strong function of the Reynolds number. Dolling and Bogdonoff[4] report that the flowfields generated by circular cylinders and hemicylindrically blunted fins are very similar ahead of the protuberances. They also report that the protuberance height-to-diameter ratio is the relevant parameter for the generation of the asymptotic result, which occurs when increases in protuberance height do not change the interaction properties. Protuberances giving rise to the asymptotic result are called semi-infinite. The flow region upstream of the protuberances has received most of the attention in the previous studies of the flow. Dolling and Bogdonoff[5] and Fomison and Stollery[6] present some data for the downstream development of the flow in blunt-fin induced interactions. The report by Couch[7] is probably the only reference presenting data for the development of the flow downstream of a cylinder.

This Note describes an experimental investigation of the shock-wave/turbulent boundary-layer interaction induced by a cylindrical protuberance at Mach numbers 1.7 and 2.2. Data are presented for flow regions both upstream and downstream of the cylinder. Various physical aspects of the flow are illuminated by the experimental data, which include the static pressure contours and the topology of the skin-friction lines on the flat plate. Yüceil[8] gives a detailed description of the study and presentation of results.

Experiments

The experiments were carried out in the 60- × 30-mm trisonic wind tunnel at the Istanbul Technical University in Turkey. This facility is a continuous tunnel operating at atmospheric stagnation conditions. The freestream Mach number M was varied by changing the shape of the Laval nozzle upstream of the test section. The freestream Reynolds number per meter length was 14.7×10^6 (1/m) and 12.0×10^6 (1/m) at Mach 1.7 and 2.2, respectively.

The circular cylinders used in the study were made of aluminum and were mounted on the centerline of the 60-mm-wide sidewall of the tunnel. The sidewall was perpendicular to the nozzle contour. The wetted length of the tunnel sidewall from

Received Feb. 14, 1991; revision received July 10, 1991; accepted for publication July 11, 1991. Copyright © 1991 by the American Institute of Aeronautics and Astronautics, Inc. All rights reserved.

*Associate Professor, Department of Aeronautics and Astronautics.

†Graduate Student, Department of Aeronautics and Astronautics; currently at University of Texas, Austin, TX 78712.